
**MATHEMATICAL STUDY OF TWO-DIMENSIONAL TEMPERATURE
VARIATION IN TUMOR EMBEDDED BREAST TISSUE**

SHARMILA SHRESTHA¹, GOKUL K.C.² AND DIL BAHADUR GURUNG³

^{1,2,3} *Department of Mathematics, School of Science, Kathmandu University, Nepal*

Abstract: The human body is made by 100 trillion cells. The uncontrolled and abnormal growth of cells causes tumors. Due to the presence of tumor, the skin surface temperature of body provides abnormal behavior than normal. Most of the breast tumor develops in lobules and milk ducts of glandular layer. In this study, tumor is assumed in glandular layer. The study of this work is focused to find the temperature distribution in tumor embedded female breast tissue with different tumor location and different tumor size. For this, the finite element method is used to solve two-dimensional Pennes bioheat equation. The results show that the skin surface temperature of breast is higher with nearest tumor from areola. The temperature variation in breast tissue with tumors located at symmetrical position about the central line of the breast are identical.

Key Words: Breast tumor, Temperature variation, FEM.

AMS (MOS) Subject Classification. 92C35, 80A20, 35Q79.

Received: October, 2020 Accepted: March 24, 2021 Published Online: June 30, 2021

1. INTRODUCTION

The human body is made by 100 trillion cells [5], which can survive for months or years. When these cells are died or are damaged, they are replaced by new one. During their life cycle, the cell is divided into two new cells. When cell division is uncontrolled, the cell is divided into more than two cells. The uncontrolled and abnormal growth of cells causes tumors. The main two types of tumors are benign and malignant. Benign tumors are not dangerous to health. They don't spread to other parts of the body. But malignant tumors are cancerous, aggressive, and spread to other parts of the body. Blood perfusion and metabolic rate are high in tumor due to fulfilling needs of more nutrition for growth. Breast tumor develops in the cell of breast tissue. It causes the abnormal temperature variation in the breast tissue.

Sudharsan and Ng [19] developed a two-dimensional model of surface temperature distribution of female breast with and without tumor. Saxena and Pardasani [15], Pardasani and Adlakha [12] studied the problems involving tumor in skin and subcutaneous tissue (SST) regions of human body. Lawson and Chughtai [7] established the regional temperature difference of breast skin surface with increased blood perfusion and increased metabolism in

tumor. Makrariya and Pardasani [8] numerically studied on the heat transfer in uniformly perfused tumor of female breast tissue during menstrual cycle under cold environment. Xu et al. [20] described the temperature distribution in tumor and surrounding healthy tissue in cancer treatment.

Shrestha et al. [16, 17] studied one-dimensional finite element method on thermal analysis of female breast tissue with different size and location of tumor. They studied the temperature variation of breast tissue with tumor on central line of the breast only. The present paper is the extension of one-dimensional work of Shrestha et al. [16, 17] to two-dimensional, which provides the more realistic in geometric structure and physical phenomena of the breast tissue. In this work, tumor's position is located at different part of the glandular layer (not only central line) of the breast with different size and find the temperatures of tumorous breast tissue. The aim of the study is to solve two-dimensional Pennes bioheat equation for temperature variation of tumor embedded female breast tissue using finite element method.

2. MODEL FORMULATION

The breast is hemi-spherical shape with five main layers: epidermis, dermis, subcutaneous tissue, glandular layer and muscle with thoracic wall. The domain of the breast is assumed to be 72 mm from areola to the body core [9, 10, 11, 16, 17] with thickness of epidermis, dermis, subcutaneous tissue, glandular layer and muscle with thoracic wall are taken 1.5 mm, 2 mm, 1.5 mm, 45 mm and 22 mm, respectively. X-axis is central line of the breast. The part of the breast is symmetrical about the central line. Most of the breast tumor develops in lobules and milk ducts of glandular layer. So, tumor is assumed in glandular layer in the study. Figure 1 represents the schematic diagram of two-dimensional discretization of breast tissue with tumors T_1, T_2, T_3, T_4 and T_5 . The diameter of tumors T_1, T_2, T_3 is taken 20 mm and for tumors T_4 and T_5 is 10 mm. Tumor T_2 is assumed at central line of the breast and tumors T_1, T_3 exist in opposite direction and parallel to the central line of the breast at equi-distance from tumor T_2 . Tumors T_4 and T_5 lie on the central line of the breast at different positions. The center of tumors T_1, T_2, T_3, T_4 and T_5 are (35, 0), (35, 37), (35, -37), (10, 0) and (35, 0), respectively. T_2 and T_4 are concentric tumors with different size.

2.1. Governing Equation: For numerical solution, Pennes bioheat equation [14] of two-dimensional model is used, which describes the energy balance between metabolism and blood perfusion in a living tissue. The simplified form of bioheat equation is:

$$(2.1) \quad K \Delta T + P (T_b - T) + M_h + M_t = 0$$

where, K is thermal conductivity of tissue [$W/m \text{ } ^\circ C$], $\Delta = \nabla^2$ is Laplacian operator, $P = w_b c_b \rho_b$ [$W/m^3 \text{ } ^\circ C$], w_b is volumetric blood perfusion rate per unit volume [s^{-1}], c_b is specific heat of the blood [$J/kg \text{ } ^\circ C$], ρ_b is density of the blood [kg/m^3], T_b is arterial blood temperature [$^\circ C$], T is local temperature of tissue [$^\circ C$], M_h is metabolic heat generation rate of healthy tissue [W/m^3] and M_t is extra heat generation due to tumor [W/m^3]. $M_t = 0$ for normal breast tissue.

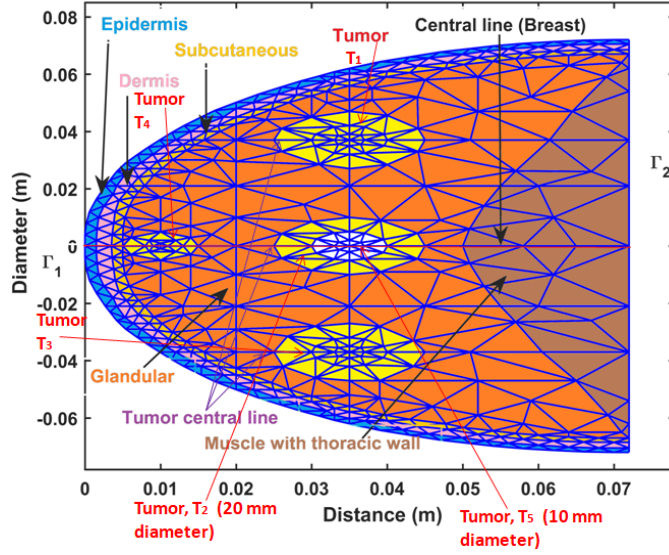


FIGURE 1. Schematic diagram of 2-D discretization of breast tissue with tumors.

2.2. Boundary Condition: Skin is the outer surface of the breast, which is in direct contact with the environment. Heat loss from skin is caused by convection, radiation and sweat evaporation. The mixed boundary condition [3, 16] is used in outer surface of the breast:

$$(2.2) \quad \Gamma_1 : K \frac{\partial T}{\partial \eta} = h_c(T - T_R) + LE$$

where, η is the normal direction to the surface boundary, h_c is combined heat transfer coefficient due to convection and radiation [$W/m^2 \text{ } ^\circ C$], T_R is room temperature [$^\circ C$], L is Latent heat of evaporation [J/kg] and E is sweat evaporation rate [$kg/m^2 sec$]. The boundary condition 2.2 can be written as:

$$(2.3) \quad \Gamma_1 : K \frac{\partial T}{\partial \eta} + h T = g, \quad h > 0$$

where, $h = -h_c$, $g = -h_c T_R + LE$.

Thoracic wall is attached with body core, where the temperature is maintained at $37^\circ C$. So the Dirichlet boundary condition is used in inner part of breast:

$$(2.4) \quad \Gamma_2 : S, \quad S = 37^\circ C$$

For continuity, the temperatures at the interface of breast tissue layers are defined as:

$$(2.5) \quad K_i \frac{\partial T_i}{\partial \eta} = K_{i+1} \frac{\partial T_{i+1}}{\partial \eta}$$

$$T_i = T_{i+1}$$

2.3. Existence and Uniqueness of weak solution of Model Equation: The governing equation is:

$$(2.6) \quad -K \Delta T + PT = f \quad \text{in } \Omega$$

where, $f = P T_b + M_h + M_t$

With Boundary conditions:

$$(2.7) \quad K \frac{\partial T}{\partial \eta} + h T = g \quad \text{on } \Gamma_1$$

$$(2.8) \quad T_b = S \quad \text{on } \Gamma_2$$

$$\partial\Omega = \Gamma_1 \cup \Gamma_2, \quad \Gamma_1 \cap \Gamma_2 = \phi$$

Let $H^1(\Omega)$ be Hilbert space [2] defined as:

$$H^1(\Omega) = \{u \in L^2(\Omega) : \frac{\partial u}{\partial x_j} \in L^2(\Omega), j = 1, 2, \dots, n\}$$

with norm

$$\|u\|_{H^1(\Omega)} = \left(\int_{\Omega} |u|^2 + \int_{\Omega} |u'|^2 \right)^{1/2}$$

where,

$$L^2(\Omega) = \{u : \Omega \rightarrow \mathbb{R} | u \text{ is measureable and } \int_{\Omega} |u|^2 < \infty\}$$

with norm

$$\|u\|_{L^2(\Omega)} = \left(\int_{\Omega} |u(x)|^2 dx \right)^{1/2}$$

Define $V = \{v \in H^1(\Omega) | v = 0 \text{ on } \Gamma_2\}$ with inner product [4]

$$(2.9) \quad (u, v)_V = \int_{\Omega} (uv + \nabla u \cdot \nabla v), \text{ for all } u, v \in V$$

Assume that $T = w + G$, where $G \in H^1(\Omega)$ is a function such that $G = S$ on Γ_2 , and $S \in H^{\frac{1}{2}}(\Gamma_2)$ [4, 6],

where,

$$H^{\frac{1}{2}}(\Gamma_2) := tr(H^1(\Omega)) := \{G \in H^1(\Omega) | tr(G) = S\}$$

Here, $w = T - G$. So, $w = 0$ on Γ_2 and $w \in V$.

Multiplying (2.6) with the test function $v \in V$ and integrating over the domain Ω yields

$$(2.10) \quad K \int_{\Omega} \nabla w \cdot \nabla v + P \int_{\Omega} w v + h \int_{\Gamma_1} w v = \int_{\Omega} f v - K \int_{\Omega} \nabla G \cdot \nabla v \\ - P \int_{\Omega} G v - h \int_{\Gamma_1} G v + \int_{\Gamma_1} g v$$

Thus, the weak form or variational problem of governing equation (2.6) is:

find $T = w + G$, $w \in V$ such that

$$(2.11) \quad a(w, v) = \ell(v) \text{ for all } v \in V$$

where,

$$\begin{aligned} a(w, v) &= K \int_{\Omega} \nabla w \cdot \nabla v + P \int_{\Omega} w v + h \int_{\Gamma_1} w v \\ \ell(v) &= \int_{\Omega} f v - K \int_{\Omega} \nabla G \cdot \nabla v - P \int_{\Omega} G v - h \int_{\Gamma_1} G v + \int_{\Gamma_1} g v \end{aligned}$$

(i) As $a(w, v) = a(v, w)$, $a(\cdot, \cdot)$ is symmetric.

(ii) for $w_1, w_2, v \in V$ and $\alpha_1, \alpha_2 \in \mathbb{R}$

$$a(\alpha_1 w_1 + \alpha_2 w_2, v) = \alpha_1 a(w_1, v) + \alpha_2 a(w_2, v)$$

and, for $w, v_1, v_2 \in V$ and $\beta_1, \beta_2 \in \mathbb{R}$

$$a(w, \beta_1 v_1 + \beta_2 v_2) = \beta_1 a(w, v_1) + \beta_2 a(w, v_2)$$

Therefore, $a(\cdot, \cdot)$ is a bilinear functional on $V \times V$.

(iii) Since $|a(w, v)| \leq C_1 \|w\|_V \|v\|_V$, $v, w \in V$, $C_1 > 0$, $a(\cdot, \cdot)$ is bounded and hence continuous.

(iv) Since $a(v, v) \geq C_2 \|v\|_{H^1(\Omega)}^2$, $v \in V$, $C_2 > 0$, $a(\cdot, \cdot)$ is Coercive or V-elliptic.

(v) $\ell(\cdot)$ is bounded since $|\ell(v)| \leq C_3 \|v\|_V$, $C_3 > 0$.

(vi) For $v_1, v_2 \in V$ and $\alpha_1, \alpha_2 \in \mathbb{R}$, $\ell(\alpha_1 v_1 + \alpha_2 v_2) = \alpha_1 \ell(v_1) + \alpha_2 \ell(v_2)$

Therefore, $\ell(\cdot)$ is linear.

Here, $a(\cdot, \cdot) : V \times V \rightarrow \mathbb{R}$, is bilinear, bounded and V-elliptic (The detail solution is given in Appendix). Also, $\ell : V \rightarrow \mathbb{R}$ is a bounded linear functional and $\ell \in V^*$, the dual space of V . Hence by the Lax-Milgram theorem, there exists a weak solution $w \in V$, which is unique. Also, $T = w + G$ exists. For uniqueness of T , assume that T_1 and T_2 are two solutions of the problem (2.11). Then,

$$a(T_1, v) = \ell(v), \quad a(T_2, v) = \ell(v), \quad \forall v \in V$$

Here, $T_1 - T_2 = w_1 + G - w_2 - G = w_1 - w_2 \in V$ (Since, $w_1 - w_2 = 0$ on Γ_2)

Then, $T_1 - T_2$ satisfies

$$\begin{aligned} T_1 - T_2 \in V, \quad a(T_1 - T_2, v) &= a(T_1, v) - a(T_2, v), \quad \forall v \in V \\ K \int_{\Omega} \nabla(T_1 - T_2) \cdot \nabla v + P \int_{\Omega} (T_1 - T_2) v + h \int_{\Gamma_1} (T_1 - T_2) v &= \ell(v) - \ell(v) \end{aligned}$$

Taking $v = T_1 - T_2$,

$$K \int_{\Omega} |\nabla(T_1 - T_2)|^2 + P \int_{\Omega} |T_1 - T_2|^2 + h \int_{\Gamma_1} |T_1 - T_2|^2 = 0$$

$$\text{Thus, } \nabla(T_1 - T_2) = 0, \quad T_1 - T_2 = 0$$

$$\text{So, } T_1 = T_2$$

Therefore, T is unique.

Since $a(\cdot, \cdot)$ is symmetric, the variational problem (2.11) is equivalent to the minimization problem;

$$I[T(x, y)] = \frac{1}{2} a(T, T) - \ell(T)$$

The variational form of the partial differential Equation (2.1) together with its boundary condition (2.2) in two dimension is given by;

$$(2.12) \quad I[T(x, y)] = \frac{1}{2} \iint_{\Omega} \left[K \left(\left(\frac{\partial T}{\partial x} \right)^2 + \left(\frac{\partial T}{\partial y} \right)^2 \right) + P (T_b - T)^2 - 2MT \right] dx dy + \frac{1}{2} \int_{\Gamma_1} \left[h_c (T - T_{\infty})^2 + LET \right] d\Gamma_1$$

where, $M = M_h + M_t$

For minimization,

$$(2.13) \quad \frac{dI}{dT_i} = 0$$

where, T_i represents the temperature in i^{th} triangular mesh.

The system of equation (2.13) can be written in matrix form:

$$(2.14) \quad A T = B$$

where, $T = [T_i]$ is $N \times 1$ vector, $B = [B_i]$ is $N \times 1$ load vector matrix and A is $N \times N$ Conductance matrix respectively, N is the total number of nodal points in discretization of the domain.

Since $a(\cdot, \cdot) : V \times V \rightarrow \mathbb{R}$, $V = H^1(\Omega)$ is symmetric and its associated bilinear form is Coercive, A is symmetric positive definite matrix. So, its eigenvalues are all positive and A is nonsingular matrix. Hence, A is invertible and the system of equation (2.14) has a unique solution:

$$(2.15) \quad T = A^{-1} B$$

2.4. Methodology: The temperature variation in tumor embedded breast has studied with different position and size of tumor. For numerical solution, whole domain of the breast is divided into 862 triangular finite elements. The epidermal, dermal and subcutaneous layers of SST region are divided into 128, 128, 130 triangular finite elements, respectively. The glandular layer with tumor and muscle with thoracic wall are divided into 434 and 42 triangular finite elements, respectively. Tumors T_1 , T_2 , T_3 are divided into 52 triangular finite elements. Tumors T_4 and T_5 are divided into 28 triangular finite elements. Tumors are assumed to be uniformly perfused tissue. The parameter values used in model are shown in Tables 1 and 2.

3. RESULTS AND DISCUSSION

Figure 2 presents the temperature profile of the breast tissue at different tumor position. Tumor T_2 is located at central line of the breast. The results show that the temperature of breast tissue increases from breast surface to the tumor region due to high blood perfusion in tumor, then steady state to the body core, which meets the realistic phenomena of the human body. The body core temperature of human body is assumed to be maintained at $37^\circ C$ and environment temperature is assumed at $25^\circ C$. Since environment temperature is less than body core temperature, the temperature of the breast tissue is continuously

TABLE 1. Values of thermal conductivity, perfusion and metabolism

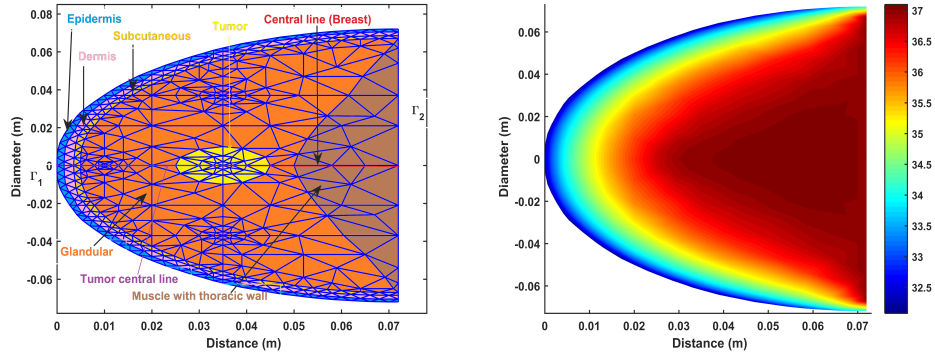
Layers of Breast Tissue	Thermal Conductivity K ($W/m\ ^\circ C$)	Perfusion $w_b\ c_b\ \rho_b$ ($W/m^3\ ^\circ C$)	Metabolism M (W/m^3)
Epidermis	0.20934 [1, 16, 17]	0 [1, 16, 17]	0 [1, 16, 17]
Dermis	0.31401 [1, 16, 17]	800 [16, 17]	400 [16, 17]
Subcutaneous	0.41868 [1, 16, 17]	800 [9, 16, 17, 19]	400 [9, 16, 17, 19]
Glandular	0.48 [9, 16, 17, 19]	2400 [9, 16, 17, 19]	700 [9, 16, 17, 19]
Muscle with Thoracic wall	0.48 [9, 16, 17, 19]	2400 [9, 16, 17, 19]	700 [9, 16, 17, 19]
Tumor	0.55 [18]	48000 [9, 16, 17, 19]	1400 [16, 17, 19]

TABLE 2. Parameter values used in Model

Parameters	Values	Units	Source
Density of tissue (ρ)	1050	kg/m^3	[1, 16, 17]
Specific heat of tissue (c)	3475.044	$J/kg\ ^\circ C$	[1, 16, 17]
Heat transfer coefficient (h_c)	13.5	$W/m^2\ ^\circ C$	[11, 17, 19]
Latent heat of evaporation (L)	2.4×10^6	J/kg	[1, 16, 17]
Sweat evaporation rate (E)	3.0806×10^{-6}	$kg/m^2\ sec$	[13]
Room temperature (T_R)	25	$^\circ C$	[13]
Body core temperature (T_b)	37	$^\circ C$	[16, 17, 19]

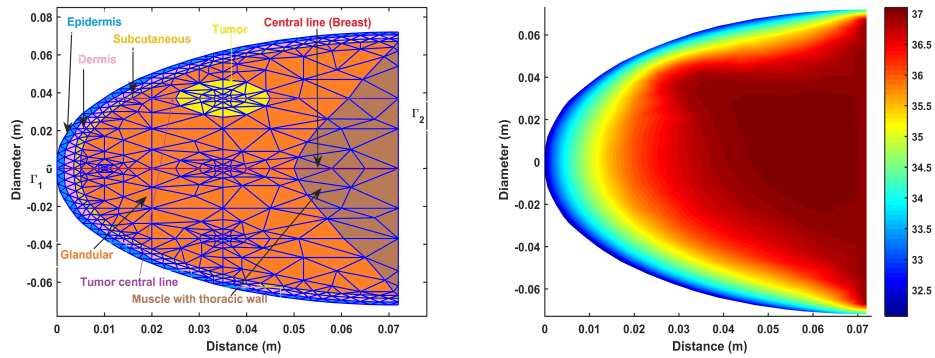
increasing from the skin surface to the tumor region and maintains deep tissue temperature [17]. The similar behavior of the temperature in tumors T_1 and T_3 are shown in Figures 3 and 4 respectively. It is observed from the Figures 5 and 6 that when the tumor size is taken 10 mm, temperature of the breast tissue increases from breast surface to the body core due to small size of tumor.

Figure 7 represent the temperature profiles of the breast tissue with tumor size 20 mm. Figure 7(b) presents the temperature profiles of the central line of the breast. The results show that the temperature of tumor T_2 is higher than tumors T_1 and T_3 because tumor T_2 lies on the central line of the breast. The central temperature of tumor T_2 is higher than tumors T_1 and T_3 by $0.22^\circ C$. The skin surface temperature of tumor T_2 is $32.30^\circ C$. Tumors T_1 and T_3 have same skin surface temperatures $32.27^\circ C$ due to symmetric position from



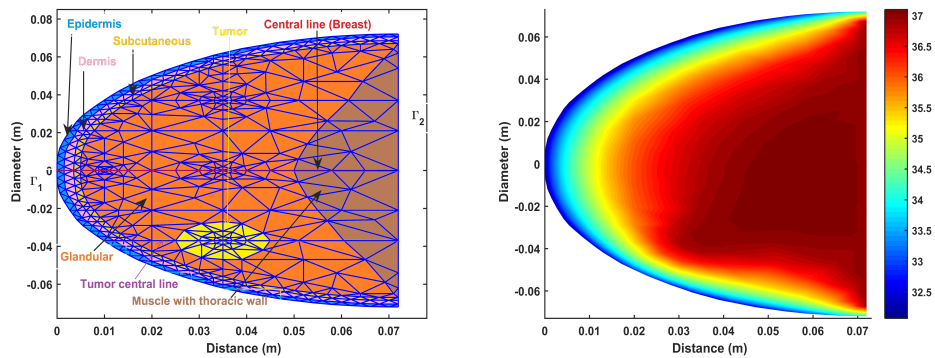
(a) Tumor T_2 at center (35, 0) in unit mm . (b) Temperature profiles of breast with tumor T_2 .

FIGURE 2. Breast tissue with tumor on central line of the breast.



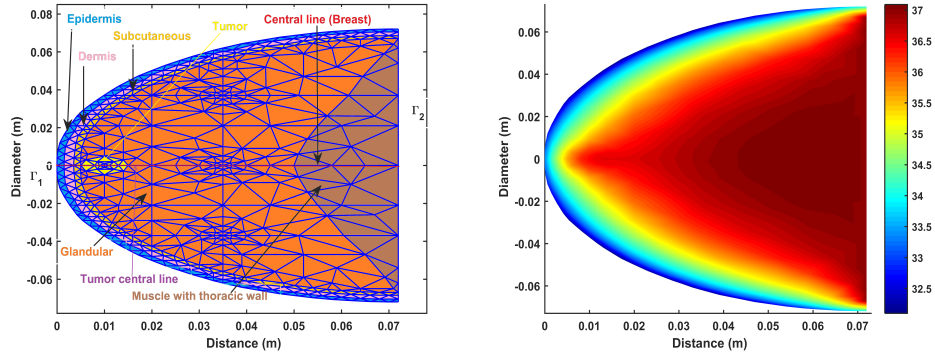
(a) Tumor T_1 at center (35, 37) in unit mm . (b) Temperature profiles of breast with tumor T_1 .

FIGURE 3. Breast tissue with tumor parallel to central line (above x-axis) of the breast.



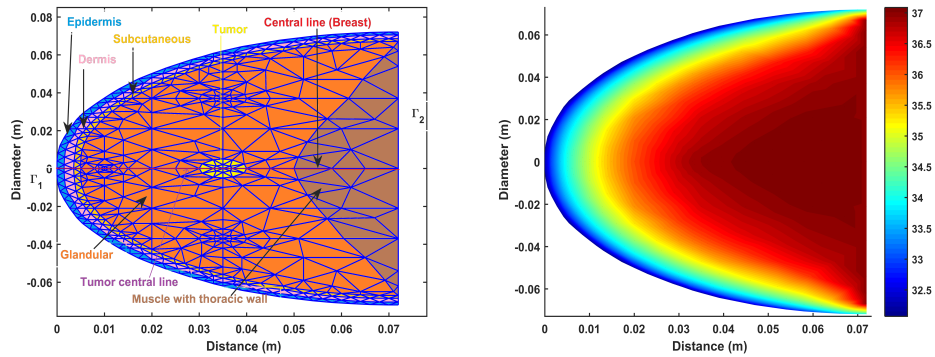
(a) Tumor T_3 at center (35, -37) in unit mm . (b) Temperature profiles of breast with tumor T_3 .

FIGURE 4. Breast tissue with tumor parallel to central line (below x-axis) of the breast.



(a) Tumor T_4 at center (10, 0) in unit mm . (b) Temperature profiles of breast with tumor T_4 .

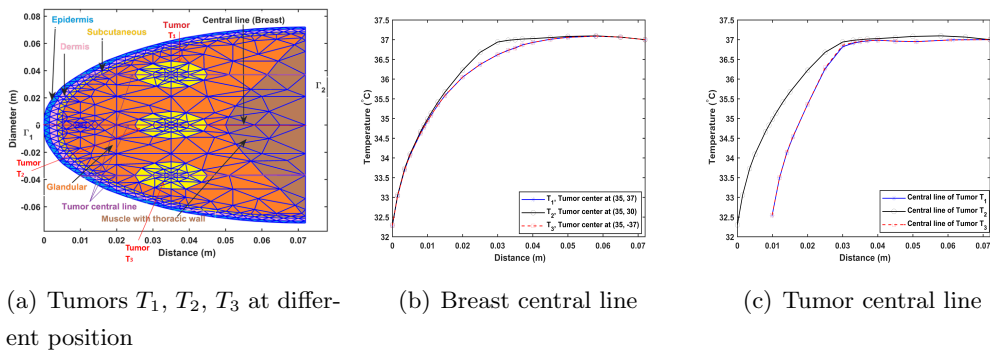
FIGURE 5. Breast tissue with tumor 10 mm far from areola at central line of the breast.



(a) Tumor T_5 at center (35, 0) in unit mm . (b) Temperature profiles of breast with tumor T_5 .

FIGURE 6. Breast tissue with tumor 35 mm far from areola at central line of the breast.

central line of the breast.

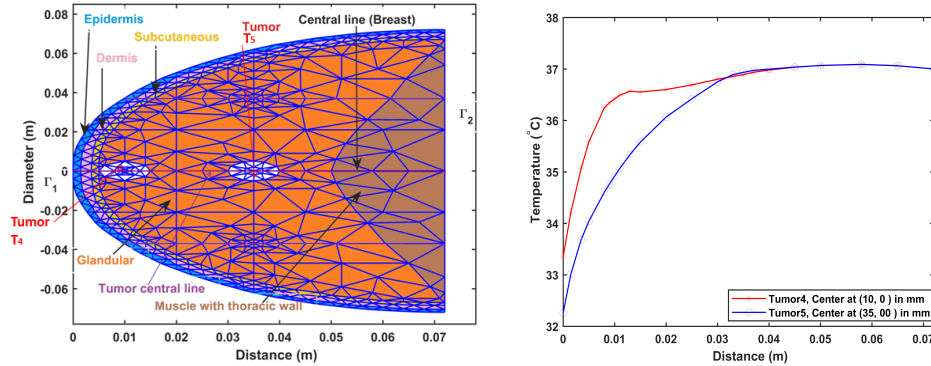


(a) Tumors T_1, T_2, T_3 at different position (b) Breast central line (c) Tumor central line

FIGURE 7. Temperature profiles of the breast tissue with tumor size 20 mm .

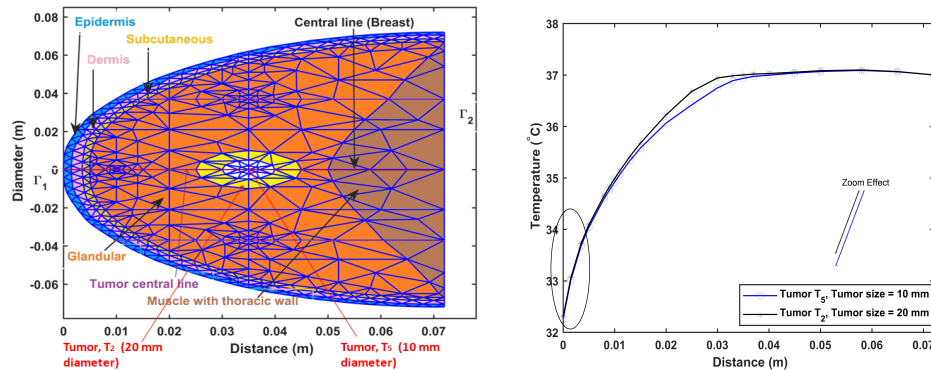
Figure 7(c) presents the temperature profiles of the central line of the tumors. The central

line of tumors T_1 and T_3 are opposite direction and parallel to the central line of the breast (i.e., x-axis) and located at a symmetrical position from tumor T_2 . The results show that the temperature of the central line of tumor having equi-distance from central line of breast are identical.



(a) Tumors T_4, T_5 at different location. (b) Temperature profiles of the breast tissue with tumors T_4 and T_5 .

FIGURE 8. Temperature profiles of the breast tissue with tumor size 10 mm.



(a) Tumors T_2, T_5 with different size (b) Temperature profiles of the breast tissue with tumor T_2, T_5 .

FIGURE 9. Temperature profiles of the breast tissue with different tumor size.

The temperature profiles of the breast tissue with tumors T_4 and T_5 are shown in Figure 8. Tumors T_4 and T_5 with tumor size 10 mm are located at distance 10 mm and 35 mm, respectively from areola. The exhibited graphs show that the temperature of breast tissue with tumor T_4 is higher than T_5 . The skin surface temperature of breast tissue with tumors T_4 is higher than T_5 by $1.09^\circ C$ because tumor T_4 is nearest to areola than T_5 .

Figure 9 exhibits the temperature profile of the breast tissue with different tumor size. There are two concentric tumors T_5 and T_2 with different tumor size 10 mm and 20 mm, respectively, located at center (35, 0). Tumor T_2 covers a large area of the breast than tumor T_5 which causes the tumor T_2 nearest from areola than tumor T_5 . The results show

that the temperature in tumor T_2 is higher than tumor T_5 due to smaller size of tumor T_5 . The skin surface temperature of breast tissue with tumor T_2 is higher than tumor T_5 by $0.04^\circ C$ because tumor T_2 is nearest to areola than tumor T_5 . There is small variation between temperature of tumors T_2 and T_5 due to tumors position are 35 mm far from areola.

4. CONCLUSIONS

In this work, the two-dimensional bioheat equation based on steady state temperature distribution of the female breast is studied at different tumor size and location using finite element method. The temperature of tumorous breast increases from skin surface to the tumor center then steady state to the body core due to high impact of blood perfusion and metabolism in tumor. The breast tissue with symmetric position of tumor from central line of the breast (i.e., x-axis) are identical. Tumorous breast temperature increases when tumor size increases. The skin surface temperature of breast tissue is higher with the nearest tumor from areola.

Acknowledgement

This study is funded to the first author by the University Grants Commission (UGC) Nepal, under the UGC PhD Fellowship (Award No: PhD /74 - 75/ S & T - 11). We would like to acknowledge University Grants Commission, Nepal.

The authors would like to acknowledge all anonymous reviewers and editors for their many insightful comments and suggestions for the improvement of the paper.

REFERENCES

- [1] S. Acharya, D.B. Gurung, and V. P. Saxena, Effect of Metabolic Reaction on Thermoregulation in Human Males and Females Body, *Journal of Applied Mathematics*, Vol. 4, pp 39 - 48, 2013.
- [2] H. Brezis, Functional Analysis, Sobolev Spaces and Partial Differential Equations, *Springer, New York*, pp 89 - 140, 2011.
- [3] D. B. Gurung, K. C. Gokul, and P. R. Adhikary, Mathematical Model of Thermal Effects of Blinking in Human Eye, *International Journal of Biomathematics*, Vol. 9, no. 1, pp 1 - 20, 2016, DOI: 10.1142/S1793524516500066.
- [4] M. S. Gockenbach, Understanding and Implementing the Finite Element Method, *SIAM, Society for Industrial and Applied Mathematics, Philadelphia*, pp 45 - 110, 2006, ISBN: 978-0-89871-614-6.
- [5] C. Guyton and E. Hall, Text Book of Medical Physiology, *Elsevier, Philadelphia*, 14 th Edition, pp 11, 2020.
- [6] S. Kesavan, Topics in Functional Analysis and Applications, *New Age International Publishers*, pp 120, 2015, ISBN-13 : 978-8122437973.
- [7] R. N. Lawson and M. S. Chughtai, Breast Cancer and Body Temperatures, *Canadian Medical Association Journal*, Vol. 88, pp 68 - 70, 1963.
- [8] A. Makrariya and K. R. Pardasani, Numerical study of the effect of non-uniformly Perfused Tumor on Heat Transfer in Women's Breast during Menstrual cycle under Cold Environment, *Network Modeling Analysis in Health Informatics and Bioinformatics*, Vol. 8, no. 9, pp 1 - 7, 2019, DOI: 10.1007/s13721-019-0189-1.

- [9] M. Mital and R. M. Pidaparti, Breast Tumor Simulation and Parameters Estimation Using Evolutionary Algorithms, *Hindawi Publishing Corporation Modelling and Simulation in Engineering*, Vol. 2008, pp 1 - 6, 2008, Article ID 756436, DOI: 10.1155/2008/756436.
- [10] E. Y. K. Ng and N. M. Sudarshan, An Improved Three-Dimensional direct numerical Modeling and Thermal Analysis of a Female Breast with Tumor, *Proceedings of the Institution of Mechanical Engineers.Part H, Journal of Engineering in Medicine*, Vol. 215, no. 1, pp 25 - 37, 2001.
- [11] M. M. Osman and E. M. Afify, Thermal Modeling of the Normal Woman's Breast, *Journal of Biomechanical Engineering*, Vol. 106, no. 2, pp 123 - 130, 1984. [PubMed: 6738016].
- [12] K. R. Pardasani and N. Adlakha, Exact solution to a heat flow problem in peripheral tissue layers with a solid tumor in the dermis, *Ind. J. Pure. Appl. Math.*, Vol. 22, no. 8, pp 679 - 687, 1991.
- [13] S. J. Park and T. Tamura, Distribution of Evaporation Rate on Human Body Surface, *Ann. Physiol. Anthropol.*, Vol. 11, no. 6, pp 593 - 609, 1992.
- [14] H. H. Pennes, Analysis of tissue and arterial blood temperature in resting forearm, *Journal of applied physiology*, Vol. 1, pp 93 - 122, 1948.
- [15] V. P. Saxena and K. R. Pardasani, Effect of dermal tumor on temperature distribution in skin with variable blood flow, *Bull Math. Bio., U.S.A.*, Vol. 53, no. 4, pp 525 - 536, 1991.
- [16] S. Shrestha, K.C. Gokul, and D. B. Gurung, Transient Bioheat Equation in Breast Tissue: Effect of Tumor Size and Location, *Journal of Advances in Applied Mathematics*, Vol. 5, no. 1, pp 9 - 19, 2020, DOI: 10.22606/jaam.2020.51002.
- [17] S. Shrestha and D. B. Gurung, Finite Element Method Approach for Thermal Analysis of Female Breast Tissue Tumor Model, *J Appl bioinforma Comput Biol*, Vol. 6, no. 3, pp 1 - 6, 2017, DOI: 10.4172/2329-9533.1000141.
- [18] S. Soni, H. Tyagi, R. A. Taylor, and A. Kumar, The Influence of Tumour Blood Perfusion Variability on Thermal Damage During Nanoparticle Assisted Thermal Therapy, *International Journal of Hyperthermia*, Vol. 31, no. 6, pp 615 - 625, 2015, DOI: 10.3109/02656736.2015.1040470.
- [19] N. M. Sudarshan and E. Y. K. Ng, Surface Temperature Distribution of a Breast with and without Tumour, *Computer Methods in Biomechanics and Biomedical Engineering*, Vol. 2, no. 3, pp 187 - 199, 1999, [PubMed: 11264827].
- [20] Y. Xu, S. Long, Y. Yang, F. Zhou, N. Dong, K. Yan, B Wang, Y. Zeng, N. Du, X. Li and W. R. Chen, Mathematical simulation of Temperature Distribution in Tumor Tissue and surrounding Healthy Tissue treated by Laser combined with Indocyanine green, *Theoretical Biology and Medical Modelling*, Vol. 16, no. 12, pp 1 - 11, 2019, DOI: 10.1186/s12976-019-0107-3.

APPENDIX

For $a(\cdot, \cdot)$ symmetric

$$\begin{aligned}
 a(w, v) &= K \int_{\Omega} \nabla w \cdot \nabla v + P \int_{\Omega} w v + h \int_{\Gamma_1} w v \\
 &= K \int_{\Omega} \nabla v \cdot \nabla w + P \int_{\Omega} v w + h \int_{\Gamma_1} v w \\
 &= a(v, w)
 \end{aligned}$$

Therefore, $a(\cdot, \cdot)$ is symmetric.

For $\mathbf{a}(\cdot, \cdot)$ bilinear

(i) for $w_1, w_2, v \in V$ and $\alpha_1, \alpha_2 \in \mathbb{R}$

$$\begin{aligned}
a(\alpha_1 w_1 + \alpha_2 w_2, v) &= K \int_{\Omega} \nabla(\alpha_1 w_1 + \alpha_2 w_2) \cdot \nabla v + P \int_{\Omega} (\alpha_1 w_1 + \alpha_2 w_2) v \\
&\quad + h \int_{\Gamma_1} (\alpha_1 w_1 + \alpha_2 w_2) v \\
&= \alpha_1 \left(K \int_{\Omega} \nabla w_1 \cdot \nabla v + P \int_{\Omega} w_1 v + h \int_{\Gamma_1} w_1 v \right) \\
&\quad + \alpha_2 \left(K \int_{\Omega} \nabla w_2 \cdot \nabla v + P \int_{\Omega} w_2 v + h \int_{\Gamma_1} w_2 v \right) \\
&= \alpha_1 a(w_1, v) + \alpha_2 a(w_2, v)
\end{aligned}$$

(ii) For $w, v_1, v_2 \in V$ and $\beta_1, \beta_2 \in \mathbb{R}$

$$\begin{aligned}
a(w, \beta_1 v_1 + \beta_2 v_2) &= K \int_{\Omega} \nabla w \cdot \nabla(\beta_1 v_1 + \beta_2 v_2) + P \int_{\Omega} w (\beta_1 v_1 + \beta_2 v_2) \\
&\quad + h \int_{\Gamma_1} w (\beta_1 v_1 + \beta_2 v_2) \\
&= \beta_1 \left(K \int_{\Omega} \nabla w \cdot \nabla v_1 + P \int_{\Omega} w v_1 + h \int_{\Gamma_1} w v_1 \right) \\
&\quad + \beta_2 \left(K \int_{\Omega} \nabla w \cdot \nabla v_2 + P \int_{\Omega} w v_2 + h \int_{\Gamma_1} w v_2 \right) \\
&= \beta_1 a(w, v_1) + \beta_2 a(w, v_2)
\end{aligned}$$

Therefore, $a(\cdot, \cdot)$ is a bilinear functional on $V \times V$.

For $\mathbf{a}(\cdot, \cdot)$ is bounded (or continuous)

$$\begin{aligned}
|a(w, v)| &= \left| K \int_{\Omega} \nabla w \cdot \nabla v + P \int_{\Omega} w v + h \int_{\Gamma_1} w v \right| \\
&\leq K \int_{\Omega} |\nabla w \cdot \nabla v| + P \int_{\Omega} |w v| + h \int_{\Gamma_1} |w v| \\
&\leq K \|\nabla w\|_{L^2(\Omega)} \|\nabla v\|_{L^2(\Omega)} + P \|w\|_{L^2(\Omega)} \|v\|_{L^2(\Omega)} + h \|w\|_{L^2(\Gamma_1)} \|v\|_{L^2(\Gamma_1)} \\
&\quad (\because \text{By Cauchy-Schwarz inequality [4]})
\end{aligned}$$

Since

$$\begin{aligned}
\|\nabla w\|_{L^2(\Omega)}^2 &= \int_{\Omega} \nabla w \cdot \nabla w \leq \int_{\Omega} (w^2 + \nabla w \cdot \nabla w) = \|w\|_V^2 \\
\|w\|_{L^2(\Omega)}^2 &= \int_{\Omega} w^2 \leq \int_{\Omega} (w^2 + \nabla w \cdot \nabla w) = \|w\|_V^2
\end{aligned}$$

and similarly for v , it follows that

$$\begin{aligned}
|a(w, v)| &\leq K \|w\|_V \|v\|_V + P \|w\|_V \|v\|_V + h \|w\|_V \|v\|_V \\
&= C_1 \|w\|_V \|v\|_V, \quad C_1 = K + P + h > 0
\end{aligned}$$

Therefore, $a(\cdot, \cdot)$ is a bounded and hence continuous.

For $a(\cdot, \cdot)$ is V-elliptic or Coercive:

We have,

$$\begin{aligned}
 a(v, v) &= \int_{\Omega} K \nabla v \cdot \nabla v + P \int_{\Omega} v v + \int_{\Gamma_1} h v v \\
 &= K \int_{\Omega} \nabla v \cdot \nabla v + P \int_{\Omega} v^2 + h \int_{\Gamma_1} v^2 \\
 &\geq K C \|v\|_{H^1(\Omega)}^2 + P \|v\|_{L^2(\Omega)}^2 + h \|v\|_{L^2(\Gamma_1)}^2, \quad v \in V \quad (\because \text{By Poincare} \\
 &\quad \text{inequality [4], } \int_{\Omega} \nabla v \cdot \nabla v \geq C \|v\|_{H^1(\Omega)}^2, \quad v \in V, \quad C > 0) \\
 &\geq C_2 \|v\|_{H^1(\Omega)}^2, \quad v \in V, \quad C_2 = KC
 \end{aligned}$$

So, $a(\cdot, \cdot)$ is Coercive or V-elliptic.

For $\ell(\cdot)$ is bounded

we have,

$$\begin{aligned}
 |\ell(v)| &= \left| \int_{\Omega} f v dx - K \int_{\Omega} \nabla G \cdot \nabla v - P \int_{\Omega} G v - h \int_{\Gamma_1} G v + \int_{\Gamma_1} g v \right| \\
 &\leq \int_{\Omega} |f v| dx + K \int_{\Omega} |\nabla G \cdot \nabla v| + P \int_{\Omega} |G v| + h \int_{\Gamma_1} |G v| + \int_{\Gamma_1} |g v| \\
 &\leq \|f\|_{L^2(\Omega)} \|v\|_{L^2(\Omega)} + K \|\nabla G\|_{L^2(\Omega)} \|\nabla v\|_{L^2(\Omega)} + P \|G\|_{L^2(\Omega)} \|v\|_{L^2(\Omega)} \\
 &\quad + h \|G\|_{L^2(\Gamma_1)} \|v\|_{L^2(\Gamma_1)} + g \|v\|_{L^2(\Gamma_1)} \\
 &\quad (\because \text{by Cauchy-Schwarz inequality}) \\
 &\leq \xi \|v\|_V + K \|v\|_V \|G\|_V + P \|G\|_V \|v\|_V + h \|G\|_V \|v\|_V + g \|v\|_V \\
 &= C_3 \|v\|_V, \quad C_3 = \xi + (K + P + h) \|G\|_V + g
 \end{aligned}$$

since,

$$f \in L^2(\Omega), \quad \|f\|_{L^2(\Omega)} = \left(\int_{\Omega} |f| \right)^{1/2} \leq \xi, \quad \xi > 0$$

Thus, $\ell(\cdot)$ is bounded.

For linearity of $\ell(\cdot)$

For $v_1, v_2 \in V$ and $\alpha_1, \alpha_2 \in \mathbb{R}$,

$$\begin{aligned}
\ell(\alpha_1 v_1 + \alpha_2 v_2) &= \int_{\Omega} f(\alpha_1 v_1 + \alpha_2 v_2) dx - K \int_{\Omega} \nabla G \cdot (\alpha_1 \nabla v_1 + \alpha_2 \nabla v_2) \\
&\quad - P \int_{\Omega} G (\alpha_1 v_1 + \alpha_2 v_2) - h \int_{\Gamma_1} G (\alpha_1 v_1 + \alpha_2 v_2) \\
&\quad + \int_{\Gamma_1} g (\alpha_1 v_1 + \alpha_2 v_2) \\
&= \alpha_1 \left(\int_{\Omega} f v_1 dx - K \int_{\Omega} \nabla G \cdot \nabla v_1 - P \int_{\Omega} G v_1 - h \int_{\Gamma_1} G v_1 + \int_{\Gamma_1} g v_1 \right) \\
&+ \alpha_2 \left(\int_{\Omega} f v_2 dx - K \int_{\Omega} \nabla G \cdot \nabla v_2 - P \int_{\Omega} G v_2 - h \int_{\Gamma_1} G v_2 + \int_{\Gamma_1} g v_2 \right) \\
&= \alpha_1 \ell(v_1) + \alpha_2 \ell(v_2)
\end{aligned}$$

$\therefore \ell(\cdot)$ is linear.